



Photooxidation of cyclohexene in the presence of SO₂: SOA yield and chemical composition

Shijie Liu^{1,2,3}, Long Jia², Yongfu Xu², Narcisse T. Tsona¹, Shuangshuang Ge², Lin Du^{3,1,2}

¹Environment Research Institute, Shandong University, Jinan, 250100, China

5 ²State Key Laboratory of Atmospheric Boundary Layer Physics and Atmospheric Chemistry, Institute of Atmospheric Physics, Chinese Academy of Sciences, Beijing, 100029, China

³Shenzhen Research Institute, Shandong University, Shenzhen, 518057, China

Correspondence to: Lin Du (lindu@sdu.edu.cn); Yongfu Xu (xyf@mail.iap.ac.cn)

Abstract. Secondary organic aerosol (SOA) formation from cyclohexene/NO_x system with various SO₂ concentrations under UV light was studied to understand the effects of cyclic alkenes on the atmospheric environment in polluted urban areas. A clear decrease at first and then increase of the SOA yield was found with increasing SO₂ concentrations. The lowest SOA yield was obtained when initial SO₂ concentration was in the range of 30-40 ppb, while higher SOA yield compared to that without SO₂ could not be obtained until the initial SO₂ concentration was higher than 85 ppb. SOA formation was enhanced by the acid-catalyzed heterogeneous reactions, which lead to an increase in the total organic aerosol mass. The competitive reaction of OH radicals with SO₂ and VOCs was the reason for the SOA yield decrease even under acidic conditions. The competitive reaction was an important factor for SOA yield and it should not be neglected in photooxidation, especially when acid-catalyzed mechanism could not significantly improve SOA yield. The composition of organic compounds in SOA was measured using several complementary techniques including Fourier transform infrared (FTIR) spectrometer, ion chromatograph (IC) and electrospray ionization high-resolution quadrupole mass spectrometer (ESI-HR-MS). We present the first evidence that organosulfates were produced from the photooxidation of cyclohexene in the presence of SO₂.

1 Introduction

Alkenes are widely emitted from biogenic and anthropogenic sources (Zielinska et al., 1996), and their gas-phase oxidation reactions with OH, NO₃, or O₃ are among the most important processes in the atmosphere (Atkinson, 1997). The reactions of ozone with alkenes are an important source of free radicals in the lower atmosphere, which influences the oxidative capacity of the atmosphere (Paulson and Orlando, 1996). Some of the products have sufficiently low vapor pressures to condense with other gaseous species, and contribute to the secondary organic aerosol (SOA) mass (Sarwar and Corsi, 2007; Sakamoto et al., 2013; Nah et al., 2016; Jimenez et al., 2016). SOA formation from VOCs oxidation has been receiving significant attention due to its large implication in the formation of atmospheric fine particulate matter. SOA has significant impacts on



human health (Pope III and Dockery, 2006), air quality (Kanakidou et al., 2005; Jaoui et al., 2012; McFiggans et al., 2006), and global climate change (Hansen and Sato, 2001; Adams et al., 2001; Pokhrel et al., 2016).

Although cyclic alkenes widely exist in the atmosphere, their gas-phase oxidation received less attention than those of linear or branched alkenes (Sipilä et al., 2013). Cyclohexene is an important industrial chemical (Sun et al., 2013), and is also

5 widespread in urban areas (Grosjean et al., 1978). Cyclohexene has been extensively studied as a monoterpene surrogate for inferring oxidation mechanisms and aerosol formation characteristics, because it shows the basic structural unit in abundant biogenic monoterpenes and sesquiterpenes (Carlsson et al., 2012; Keywood et al., 2004). The rate constants for gas-phase reactions of cyclohexene with OH, O₃ and NO₃ were measured at room temperature to be $(6.4 \pm 0.1) \times 10^{-11}$, $(8.1 \pm 1.8) \times 10^{-17}$ and $(5.4 \pm 0.2) \times 10^{-13}$ cm³ molecule⁻¹ s⁻¹, respectively (Stewart et al., 2013; Aschmann et al., 2012). A correlation between the

10 logarithm of the rate constants and the molecular orbital energies for simple cyclic alkenes was observed. The effect of the pressure and that of the presence of SO₂ on the formation of stable gas-phase products and SOA from ozonolysis of cyclohexene were investigated (Carlsson et al., 2012). It was found that the collisional stabilization of initial clusters was an important aspect for SOA formation processes involving sulfuric acid (H₂SO₄) and organic compounds. The effect of the structure of the hydrocarbon parent molecule on SOA formation was investigated for a series of cyclic alkenes and related

15 compounds (Keywood et al., 2004). The SOA yield was found to be a function of the number of carbons present in the cyclic alkenes ring. The relative SOA yields from ozonolysis of cyclic alkenes can be quantitatively predicted from properties of the parent hydrocarbons, like the presence of a methyl group and an exocyclic double bond.

SO₂, one of the most important inorganic pollutants in urban area, plays an important role on SOA formation (Wang et al., 2005; Lonsdale et al., 2012; Liu et al., 2016). Seasonal variations of SO₂ concentrations were found to be consistent with

20 seasonal variations of PM_{2.5} concentration (Cheng et al., 2015). Smog chamber simulations have indicated that SO₂ could enhance the formation of SOA from VOCs oxidation under acidic conditions by increasing aerosol acidity and ammonium sulfate aerosol formation (Edney et al., 2005; Liu et al., 2016; Attwood et al., 2014). Anthropogenic SO₂ emissions can impact new particle formation, and SOA composition (Lonsdale et al., 2012).

Despite the existence of organosulfates in ambient aerosols was first observed in 2005 (Romero and Oehme, 2005), proper

25 identification of these aerosols was made two years later. In a series of chamber experiments studies, it was shown that organosulfates present in ambient aerosols collected from various locations mostly originate from acid-catalyzed reactions of SOA formed from photooxidation of α -pinene and isoprene (Surratt et al., 2007). Recently, substantial amount of organosulfates have been observed in SOA around the world, and organosulfates have been identified as a group of compounds which have an important contribution to the total amount of SOA in the atmosphere (Surratt et al., 2008; Froyd et al., 2010; Kristensen and Glasius, 2011; Tolocka and Turpin, 2012; Wang et al., 2015). However, the formation and

30 transformation process of organosulfates can be complex and varied, depending on the nature of the original organic compound involved. Extensive studies on their formation have been performed and several mechanisms based on a variety of reactions have been proposed. 2-Methyl-3-buten-2-ol (MBO) has been found to be an important precursor for organosulfates in the atmosphere. Smog chamber studies of OH-initiated oxidation of MBO under nitric oxide and aerosol



acidity conditions revealed the formation of organosulfates and SOA (Mael et al., 2015; Zhang et al., 2012). Chemical characterization of laboratory-generated MBO SOA revealed that an organosulfate species ($C_5H_{12}O_6S$) was formed and its formation was significantly enhanced with elevated aerosol acidity (Zhang et al., 2012). It has also been demonstrated that substantial formation of organosulfates could derive from acid-catalyzed reactive uptake of MBO-based epoxides formed during MBO photooxidation (Zhang et al., 2014). Using nuclear resonance techniques, isoprene-derived epoxides formed during isoprene photooxidation reactions were found to be important intermediates for organonitrates and organosulfates formation via potential SOA reactions (Darer et al., 2011; Hu et al., 2011). The authors further found that organonitrates could easily be transformed to organosulfates during hydrolysis in the presence of sulfate. Organosulfates formation was also found from oxidation of hydroxyhydroperoxides (Riva et al., 2016) and from heterogeneous reactions of SO_2 with selected long-chain alkenes and unsaturated fatty acids (Passananti et al., 2016).

Laboratory chamber studies showed that organosulfates were formed in the products of OH/NO_x/O₃-initiated reactions with biogenic VOCs (BVOCs), such as isoprene (Surratt et al., 2007; Surratt et al., 2008; Hatch et al., 2011), monoterpenes (Surratt et al., 2007; Gomez-Gonzalez et al., 2008; Inuma et al., 2007) and sesquiterpenes (Chan et al., 2011). Reactions with sulfates or H_2SO_4 were the main formation processes of organosulfates. Qualitative analyses of the organosulfates in SOA have been gained more attention and development (Lin et al., 2012; Shalamzari et al., 2013; Staudt et al., 2014). Riva et al. investigated the formation of organosulfates from photooxidation of polycyclic aromatic hydrocarbons and found that, in the presence of sulfate aerosol, this photooxidation was a hitherto unrecognized source of anthropogenic secondary organosulfur (Riva et al., 2015). A more complete structural characterization of polar organosulfates that originate from isoprene SOA was performed (Shalamzari et al., 2013), and an organosulfate related to methyl vinyl ketone and minor polar organosulfates related to croton aldehyde were identified. However, there was no report about the yield and chemical composition of SOA obtained from photooxidation of cyclohexene with the presence of SO_2 .

In the present work, we investigated the SOA yields and chemical composition during cyclohexene photooxidation under different SO_2 concentrations. A better understanding of the magnitude and chemical composition of SOA from different SO_2 concentrations will contribute to more accurate SOA prediction from anthropogenic sources and give valuable information related to air pollution in urban environments.

2 Methods

2.1 Chamber description

The experiments were performed in a 400 L Teflon FEP film chamber (wall thickness 125 μ m) at the Institute of Atmospheric Physics, Chinese Academy of Sciences, Beijing. The details of the chamber, including the experimental setup and analysis techniques have been described elsewhere (Du et al., 2007; Jia and Xu, 2014), and only a brief description is presented here. The reactor was surrounded by 12 black light lamps (GE F40BLB) with emission band centered at 365 nm, which were used to simulate the spectrum of the UV band in solar irradiation. Stainless steel was covered on the chamber



interior walls to maximize and homogenize the interior light intensity. Both inlet and outlet of the chamber were made of Teflon material. Atmospheric pressure was maintained in the chamber at all times. All the experiments were performed at room temperature (307 ± 2 K) under dry conditions ($RH < 10\%$). Prior to each experiment, the chamber was cleaned by purging with purified dry air for at least 8 h until residual hydrocarbons, O_3 , NO_x or particles could not be detected in the reactor. Known amounts of cyclohexene was injected into a 0.635 cm diameter Teflon FEP tube and dispensed into the chamber by purified dry air. Typical initial cyclohexene concentrations were 500 ppb. NO_x was injected by a gas-tight syringe to make the mixing ratio of NO_x in the reactor around 95 ppb during all the experiments. The mixed concentration ratios of VOCs/ NO_x were adjusted to be about 5. SOA formation experiments were carried out under UV irradiation in the presence of NO_x to produce O_3 and OH radicals for cyclohexene oxidation. Although initial VOCs, NO_x and average OH concentrations were different from typical urban conditions, efforts were made to maintain the initial concentrations of the reactants as similar as possible to make sure the effect of SO_2 was the main reason for the changes in the SOA yield. More details on the experimental conditions are shown in Table S1 of the Supplementary material.

2.2 Gas and particle measurements

Ozone concentration in the reactor was measured using ozone analyzer (Model 49C, Thermo Electron Corporation, USA). A NO - NO_2 - NO_x analyzer (Model 42C, Thermo Electron Corporation, USA) was used to monitor the NO_x concentration. Measurement of SO_2 concentration was made using a SO_2 analyzer (Model 43i-TLE, Thermo Electron Corporation, USA). The uncertainty of the O_3 , NO_x and SO_2 measurement was less than $\pm 1\%$. The detection limits of the different monitors were 0.40 ppb, 0.50 ppb, and 0.05 ppb for NO_x , O_3 , and SO_2 , respectively.

Two Tenax absorption tubes (150 mm length \times 6 mm O.D., 0.2 g sorbent) were used to collect the sample before the UV lights were turned on and at the end of each experiment, respectively. The volume of the sample was 60 mL and the sampling time was 3 min. Concentrations of cyclohexene and the main gas phase products were analyzed by thermal desorption-gas chromatography-mass spectrometry (TD-GC-MS). A thermal desorption unit (Master TD, Dani, Italy) was combined with a 6890A gas chromatograph (6890A, Agilent Tech., USA) interfaced to a 5975C mass selective detector (5975C, Agilent Tech., USA). The GC was equipped with a HP-5MS capillary column (30 m \times 0.25 mm, 0.25 μ m film thickness). The temperature program was as follows: the initial temperature of 40 $^\circ$ C was held for 4 min, and then raised to 300 $^\circ$ C at a rate of 20 $^\circ$ C min^{-1} . The inlet temperature was set at 250 $^\circ$ C and the transfer line at 200 $^\circ$ C. The ionization method in MS was electron impact ionization, and Helium was used as the carrier gas at a constant flow (1.2 mL min^{-1}). Because a very diverse range of compounds might be present in the samples, SCAN mode (36-500 amu) was used in the MS detector. This mode is known to be a classical and typical detection method for GC-MS analysis. The results were analyzed with MSD Productivity ChemStation.

Particle number concentrations and size distributions were measured with a scanning mobility particle sizer (SMPS), which consists of a differential mobility analyzer (DMA model 3081, TSI Inc., USA) and a condensation particle counter (CPC model 3776, TSI Inc., USA). A sheath flow/aerosol flow relationship of 3.0/0.3 L min^{-1} was used for the measurements. The



particle size was measured in the range of 14 to 710 nm. Each scan was 180 s. An aerosol density of 1.2 g cm^{-3} was assumed to convert the particle volume concentration into the mass concentration (Zhang et al., 2015). Size distribution data were recorded and analyzed using the TSI AIM software v9.0.

2.3 Products composition analysis

5 The chemical composition of SOA was important for analyzing the degree of VOCs oxidation, and it was used to evaluate the transformation from gas phase to particle phase. Particle phase chemical composition was studied by means of Fourier transform infrared (FTIR) spectrometer (Nicolet iS10, Thermo Fisher, USA). The aerosols were sampled through a Dekati low pressure impactor (DLPI, DeKati Ltd, Finland). The impactor was connected to a pump working at a flow rate of 10 L min^{-1} while sampling a total volume of 300 L of gas for each experimental run. Aerosols, from 108 to 650 nm diameter, were
10 collected on an ungreased zinc selenide (ZnSe) disk (25 mm in diameter) for FTIR measurements.

The characteristic bands of inorganic and organic sulfates overlap in IR spectrum. In order to distinguish between the inorganic and organic sulfates, ion chromatograph (IC, Dionex ICS-900, Thermo Fisher, USA) was used to analyze the inorganic sulfate anion (SO_4^{2-}) in SOA. SOA collected on ZnSe disks was firstly dissolved in high purity water (7 mL) and then measured by IC for SO_4^{2-} concentrations. The anions were analyzed with a Dionex IonPac AS14A analytical column
15 and an anion self-regenerating suppressor Dionex ASRS was used as eluent. The flow rate was 1.0 mL min^{-1} with a mixture of $8.0 \text{ mmol L}^{-1} \text{ Na}_2\text{CO}_3$ and $1.0 \text{ mmol L}^{-1} \text{ NaHCO}_3$ for anions analyses. The suppressing current was 50 mA.

Chemical characterization of aerosols from photooxidation of cyclohexene was performed using an electrospray ionization high-resolution quadrupole mass spectrometer (ESI-HR-MS, Thermo Fisher, USA) operated in negative (-) ion mode, which was calibrated using the manufacturer's calibration standards mixture allowing for mass accuracies $< 5 \text{ ppm}$ in external calibration mode. The ionization voltage was 4.2 kV and the capillary temperature was set at $300 \text{ }^\circ\text{C}$. N_2 was used as both
20 the sheath gas (70 U) and auxiliary gas (30 U). SOA was collected on the aluminum foil using the same method as FTIR analysis and then extracted with 1 mL of acetonitrile. The aluminum foil was used due to its ease to use and its non-reactivity with the sample. A total volume of 300 L was sampled at a flow rate of 10 L min^{-1} . A volume of $5 \text{ } \mu\text{L}$ of the extraction and a direct injection were used for the measurement. Xcalibur 2.2 software (Thermo Fisher, USA) was used for
25 the calculation of chemical formula from the accurate measurement of m/z values.

2.4 Chemicals

The chemicals used and their stated purities were as follows: cyclohexene (99%) was obtained from Aldrich and used without further purification. A zero air generator (Model 111, Thermo Scientific, USA) was used to generate clean air. The zero air has no detectable non-methane hydrocarbons (NMHC $< 1 \text{ ppb}$), NO_x ($< 1 \text{ ppb}$), low O_3 concentration ($< 3 \text{ ppb}$), and
30 low particle numbers ($< 5 \text{ cm}^{-3}$), and relative humidity (RH) below 10%. Ozone was produced from O_2 via electrical discharge using a dynamic gas calibrator (Model 146i, Thermo Scientific, USA). NO_2 (510 ppm), NO (50 ppm) and SO_2 (25 ppm) with ultra-pure N_2 (99.999%) as background gas was purchased from Beijing Huangyuan Gas Co., Ltd., China.



3 Results and discussion

3.1 Characterization of the chamber

The effective light intensity in the near ultraviolet region plays a decisive role in the formation of photochemical smog (Presto et al., 2005a). The effective light intensity of the chamber was represented by the photolysis rate constant of NO₂. In our study, the average effective light intensity was determined to be 0.177 min⁻¹.

Wall loss is the decrease of the concentration of reactive gas phase species caused by adsorption on the inner wall of the reactor. Residual reactant and product on the inner wall can also react with the gas phase species, which is another important reason for wall loss. Wall loss can directly affect the quantitative calculation of photooxidation rate and SOA yield. Correct evaluation of wall loss is therefore necessary to explain the experimental results of SOA yield. In the present study, the wall loss of cyclohexene in the chamber could be neglected. The wall loss of O₃, NO_x, and SO₂ were first order because $\ln([X]_0/[X]_t)$ had a good correlation with time ($R^2=0.994, 0.944, 0.999$ for O₃, NO_x, and SO₂, respectively). The measured wall loss rate constants for O₃, NO_x and SO₂ were 5.05×10^{-6} , 7.04×10^{-6} and $6.39 \times 10^{-6} \text{ s}^{-1}$, respectively. The average value of the wall loss rate constant of particles was $4.7 \times 10^{-5} \text{ s}^{-1}$, and the measured particle concentrations in this study were corrected using the same method as Pathak et al (Pathak et al., 2007). Typical profiles of the gas and particle phases are given in Figure S1 of the Supplementary material.

3.2 Effect of SO₂ on SOA number concentrations

The maximum particle number concentrations for cyclohexene/NO_x/SO₂ system with different initial SO₂ concentrations and the particle number concentrations at the maximum SOA yield are shown in Figure 1. After the black light lamps were turned on, SOA number concentrations increased rapidly to reach the maximum within 0.5 h in each experiment. Subsequently, the particle number concentrations gradually decreased accompanied by the growth of particle size by coagulation. The SOA mass concentration kept increasing until its maximum was reached (after ~2 h). Both types of particle number concentrations had similar trends against initial SO₂ concentrations. In general, maximum particle number concentrations were three times higher than the particle number concentrations at the maximum SOA yield. In the rest part of this paper, in order to better elaborate the effect of SO₂ on the formation of particles, the particle number concentration refers to the maximum particle number concentration.

The particle number concentration increased with initial SO₂ concentration, and this increase could be divided into two stages: increasing stage and stable stage. In the increasing stage, with the initial SO₂ concentration increasing from 0 ppb to 30 ppb, the particle number concentration grew significantly under low initial SO₂ concentration (<5 ppb), then the growth rate reduced gradually. In the stable stage, when the SO₂ concentrations were varied systematically between 30 and 105 ppb, particle number concentrations practically maintained steady (2.5×10^5 - $3.8 \times 10^5 \text{ cm}^{-3}$), and there was no obvious growth as shown in Figure 1. For experiments with high initial SO₂ concentration, the maximum particle number concentrations were 10 times of those without SO₂, indicating enhanced new particle formation (NPF) when adding SO₂. It was found that wood



soot, a minor source of SO₂ (Reddy and Venkataraman, 2002), resulted in a measurable positive deviation to the VOCs/NO_x photooxidation reaction system without background aerosol (Jang et al., 2002). Our result was consistent with a range of previous studies (Jang et al., 2002; Liu et al., 2016), in which even small amount of SO₂ could affect the new particle formation.

- 5 Nucleation is a fundamental step in the atmospheric new particle formation. Nucleation of particles in the atmosphere has been observed to be strongly dependent on the abundance of H₂SO₄ (Sihto et al., 2006; Xiao et al., 2015). Normally, SO₂ was deemed to be oxidized by OH radicals to form H₂SO₄ through homogeneous reactions in gas phase (Calvert et al., 1978), or by H₂O₂ and O₃ through in-cloud processes in aqueous phase (Lelieveld and Heintzenberg, 1992). The aqueous phase formation of H₂SO₄ is negligible in this study (RH<10%). As the precursor of H₂SO₄, SO₂ at higher concentrations would
10 lead to more H₂SO₄ formation, and thereby increase the nucleation rates and total particle number concentrations (Sipilä et al., 2010). Because of the similar initial conditions for each experiment except SO₂, the amount of OH radicals produced was assumed to be almost equal. In the presence of high concentration of SO₂, new particle formation was not enhanced. This feature may indicate that no more sulfates formed when SO₂ was in large excess (>30 ppb) and the OH radicals were insufficient. The quantity of OH radicals is the main restraint on H₂SO₄ formation at high initial SO₂ concentrations, which
15 could not lead to more H₂SO₄ formation in the present study. Therefore, the particle number concentration maintained steady, and it was independent of the SO₂ concentrations in the second stage.

Besides, the mean diameter of particles increased with photooxidation reaction time, which suggests that not many new particles were generated after a burst increase at the initial stage of SOA formation. The burst increase stage of SOA may be related to fast increase of PM_{2.5} and occurrence of haze (He et al., 2014). Once new particles are formed, there is a
20 competition between growth of existing particles by uptake of the precursors and formation of new particles. Our result agrees with previous studies that there was no obvious increase in aerosol number concentration when additional VOCs were injected, but a significant increase in SOA mass concentration (Presto et al., 2005a). Condensation onto existing aerosol particles was prior to the occurrence of new particle formation. If there was enough seed particle surface area, no new particles formation was expected to be observed.

25 3.3 Effect of SO₂ on SOA yields

SOA yield (Y) is defined as $Y = \Delta M_0 / \Delta HC$, where ΔM_0 is the produced organic aerosol mass concentration ($\mu\text{g m}^{-3}$), and ΔHC is the mass concentration of reacted cyclohexene ($\mu\text{g m}^{-3}$). The SOA yields of cyclohexene at different SO₂ concentration as determined by SMPS are shown in Figure 2. The numerical values of the aerosol mass concentration and SOA yields at different conditions are shown in Table S1 of the Supplementary material.

- 30 The SOA yields in the absence of SO₂ were in the range of 2.5% to 2.7%, which were an order of magnitude lower than those reported in previous studies (Warren et al., 2009; Keywood et al., 2004; Kalberer et al., 2000). There are three possible explanations for this phenomenon. (1) SOA formation is closely related to the oxidation capacity in the photooxidation experiments and, therefore, is affected by the ratio of $[\text{VOC}]_0 / [\text{NO}_x]_0$ (Pandis et al., 1991). Experiments performed with



different SO₂ concentrations indicate that the SOA formation is partly controlled by the ability of the system to oxidize cyclohexene and contribute to the particle mass. As indicated in Figure S2 of the Supplementary material, even at 0 ppb of SO₂, the mass concentration of SOA quickly reaches its maximum. Experiments with higher NO_x levels have been proved to get considerably lower SOA yield than those with lower NO_x levels at the same VOCs concentration (Song et al., 2005).

5 The reactions of organo-peroxy radicals (RO₂) with NO and NO₂ instead of peroxy radicals (RO₂ or HO₂) under high NO_x conditions resulted in the formation of volatile organic products and a decreased SOA yield (Lane et al., 2008). For [VOC]₀/[NO_x]₀ ratios between 3 and 10, a greater amount of nitrate radical (NO₃) was available to react with VOCs, and the NO₃-initiated reaction was a poor source of SOA, which may also contribute to the reduction of SOA yield (Presto et al., 2005b). It was reported that SOA yield was constant for [VOC]₀/[NO_x]₀>15, but decreased dramatically (by a factor of more

10 than 4) as [VOC]₀/[NO_x]₀ decreased (Presto et al., 2005b). In our study, the [VOC]₀/[NO_x]₀ ratio was maintained at about 5. Recently, the NO_x dependence of SOA formation from photooxidation of β-pinene was comprehensively investigated (Sarrafzadeh et al., 2016), and it was shown that the NO_x-induced OH concentration was the major factor influencing the SOA yield. The impacts of NO_x on SOA formation were only moderate if the impact of NO_x on OH concentration was eliminated. OH concentration in our study was relatively insufficient, which was the main limiting factor for SOA formation.

15 (2) UV light is another factor influencing the SOA yield. SOA yields between dark and UV-illuminated conditions were reported to be different (Presto et al., 2005a). Exposure to UV light could reduce SOA yield by 20%-40%, while more volatile products were formed (Griffin et al., 1999). (3) Temperature may have a pronounced influence on SOA yield (Qi et al., 2010; Emanuelsson et al., 2013). At lower temperature, semi-volatile organic compounds would favor the condensation of gas phase species and a higher SOA yield could be expected. Raising the chamber temperature by 10 K should cause a

20 decrease of 10% in aerosol yield (Pathak et al., 2007). SOA yields reported in the present study were obtained at higher temperature, 307±2 K, instead of 298 K in most previous studies. On the basis of the discussion above, SOA yield from cyclohexene in our study was lower than observed in the previous studies.

SOA yields for the cyclohexene/NO_x/SO₂ system were measured for initial SO₂ mixing ratios of 0-105 ppb. The experimental results showed a clear decrease at first and then an increase in the SOA yield with increasing SO₂

25 concentrations (Figure 2). When SO₂ concentrations increased from 0 to 40.8 ppb, there was a remarkable decrease in SOA yield with the increase of SO₂ concentration. The SOA yield dropped from 2.7% to 1.2%, reduced by 56%. For SO₂ concentrations higher than 40.8 ppb, SOA yield increased with increasing SO₂ concentration. The highest SOA yield was obtained to be 3.5%, at 104.7 ppb SO₂ concentration. The lowest SOA yield of cyclohexene photooxidation was obtained at the initial SO₂ concentration of 40 ppb. Although the SOA yield increased gradually with the initial SO₂ concentration at

30 concentrations higher than 40 ppb, a higher SOA yield than that in the absence of SO₂ could not be obtained when the initial SO₂ concentration was lower than 85 ppb.

SOA formation was enhanced by the presence of SO₂ (Jang et al., 2002), which has been previously attributed to acid-catalyzed heterogeneous reactions and produced an increase of the total organic aerosol mass (Xu et al., 2014). Even small amounts of acid are capable of catalyzing heterogeneous reactions. Both NO and NO₂ was used as NO_x for the repeated



experiments in our study. Despite the time of occurrence of the maximum SOA concentration for the experiment with NO₂ was half an hour earlier than that for the experiment with NO, the results of SOA yield were similar. However, there were some undiscovered processes in the cyclohexene/NO_x/SO₂ system that offset potential multifold increases in the SOA yield by acid-catalyzed heterogeneous reactions. The competitive reaction between SO₂ and VOCs might be the reason for the
5 decrease of the SOA yield. SO₂ could be oxidized by OH radicals to form H₂SO₄ (Somnitz, 2004). Due to the presence of O₃ in our system, the formation of Criegee intermediates and their reactions with SO₂ could be expected (Criegee, 1975). However, the importance of these reactions can be kinetically limited. The reaction of cyclohexene with ozone has a rate constant of $8.1 \times 10^{-17} \text{ cm}^3 \text{ molecule}^{-1} \text{ s}^{-1}$ (Stewart et al., 2013), considerably slower than e.g., its reaction with OH, which has a rate constant of $6.4 \times 10^{-11} \text{ cm}^3 \text{ molecule}^{-1} \text{ s}^{-1}$ (Aschmann et al., 2012). In addition to the kinetic limitation of the
10 cyclohexene reaction with O₃, the typical concentration of O₃ in our chamber was 200 ppb and hence the importance of cyclohexene reaction with O₃ was expected to be less significant than that of its reaction with OH under any relevant SO₂ conditions. The competitive reaction resulted in a decrease of the concentration of OH radicals, which was one of the main oxidizers for the photooxidation in the chamber. As mentioned above, the photooxidation in this study was at high-NO_x conditions and the OH was the main limiting factor for SOA formation because of its relatively low concentration. At lower
15 OH radical concentration condition caused by the reaction between SO₂ and OH radical, the formation of SOA was inhibited. Accordingly, SOA yield showed descending trend with the increase of SO₂ concentration when the initial SO₂ concentration was lower than 40 ppb.

When the initial SO₂ concentration was greater than 40 ppb, the acid-catalyzed heterogeneous formation of SOA became more significant (Figure 2). The lowest SOA yield was obtained at 40 ppb initial SO₂ concentration. At this concentration,
20 there was a balance between the inhibition of SOA formation by competitive reactions and the promotion by acid-catalyzed reactions. The same SOA yield was obtained in the absence of SO₂ and at 85 ppb initial SO₂ concentration. The competitive reaction plays an important role for SOA formation, and it should be taken into account in SOA simulation models or air quality models for more accurate prediction. The formation of low volatile organics (e.g. organosulfates) by photooxidation in the presence of SO₂ might be another reason for the increase of the SOA yield.

25 3.4 Organosulfates formation

When SO₂ was added into the chamber, the acidic aerosol particles were formed by photooxidation of SO₂ initiated by the reaction with OH. The amounts of SO₄²⁻ in particle phase and the consumption of SO₂ (ΔSO_2) with different initial SO₂ concentrations are shown in Figure 3. The amounts of SO₄²⁻ grew rapidly at low concentration of SO₂, but the relative growth rate dramatically decreased in the range of 20-60 ppb initial SO₂ concentrations. However, both the amount and the
30 growth rate of ΔSO_2 increased with initial SO₂ concentrations. The ratio of the amount of SO₂ for SO₄²⁻ formation to ΔSO_2 reduced gradually with the increase of initial SO₂ concentrations (Figure 3), which indicated that other products formed from SO₂ besides SO₄²⁻ in the aerosols.



Typical IR spectra of aerosols from cyclohexene/NO_x/SO₂ system under different SO₂ concentrations are presented in Figure 4. Based on the peak positions in the IR spectra, the functional groups represented by each peak are summarized as following. The broadband at 3100 to 3300 cm⁻¹ is assigned as the O–H stretching of hydroxyl and carboxyl groups (Coury and Dillner, 2008). The peak at 1717 cm⁻¹ represents the C=O stretching of aldehydes, ketones, and carboxylic acids. The peaks at 1622 and 1278 cm⁻¹ show good correlation and both are assigned to the ONO₂ stretching (Liu et al., 2012; Jia and Xu, 2014). The characteristic absorption band at 1500-1350 cm⁻¹ is the C–O stretching and O–H bending of COOH group (Ofner et al., 2011). The absorption peak of sulfate exists in the range of 1200-1000 cm⁻¹ (Wu et al., 2013). The band at 1100 cm⁻¹ in the IR spectra can be attributed to the sulfonic acid group and sulfate. It has been confirmed that the S=O absorption band in organic sulfate monoesters appears around 1040-1070 cm⁻¹ (Chihara, 1958). Although, more studies on bands assignments in organosulfates are not currently available from the literature for further comparison, the 1100 cm⁻¹ band from the current FTIR study can reasonably be assigned to S=O in sulfonic acid group.

The intensities of most absorption bands, such as O-H at 3100-3300 cm⁻¹, C=O at 1717 cm⁻¹, ONO₂ at 1622 and 1278 cm⁻¹, and C-H at 2930 cm⁻¹, have similar trends with the change of SOA yield for initial SO₂ concentrations between 11 and 105 ppb. However, the band of sulfate at 1100 cm⁻¹ in IR spectra increases with the rise of initial SO₂ concentration rather than the SOA yield, which suggests the formation of sulfonic acid group and sulfate product from SO₂ photooxidation. The relative intensity of the band at 1100 cm⁻¹ increased by 1.8 times when the initial SO₂ concentration rose from 0 to 44 ppb, whereas the band increased by 7.2 times when the initial SO₂ concentration was 105 ppb. The intensity of 1100 cm⁻¹ band grew slowly at low SO₂ concentrations due to the decrease of the formation of aerosols. To clearly show the amount of sulfonic acid group and sulfate in aerosols, the intensity of the band at 1100 cm⁻¹ and the amount of SO₄²⁻ were compared in the same aerosol mass, and are shown in Figure 5, where the amount of ΔSO₂ in the aerosols are also included. The relative intensity was set to 1 when the initial SO₂ concentration was 44.3 ppb.

With the increase of SO₂ concentration, the amount of SO₄²⁻ in unit mass of aerosols increased first and then decreased, which was negative correlation with SOA yield. However, ΔSO₂ was in a linear relationship with the initial SO₂ concentration (R²=0.94). The relative band intensities at 1100 cm⁻¹, which represented the intensity of both SO₄²⁻ and sulfonic acid group, also increased approximately in a linear form with the increase of initial SO₂ concentration (R²=0.91). If the 1100 cm⁻¹ band originated from SO₄²⁻ only, the change of the band intensity was consistent with SO₄²⁻ concentration in unit mass of aerosols. Combined with the ratio of the amount of SO₂ for SO₄²⁻ formation to ΔSO₂, it was reasonable to believe that the 1100 cm⁻¹ band originated not only from SO₄²⁻, but also from the sulfonic acid group. Organosulfates might be the products from the photooxidation of cyclohexene in the presence of SO₂ under high-NO_x conditions.

The composition of the cyclohexene SOA was examined with HR-MS using negative ion mode ESI and the mass spectrum was recorded at a resolution of 10⁵ (Figure 6). Organosulfates were identified in the particle phase from chamber experiments. Accurate mass fittings for measured ions of organosulfates in ESI negative ion mode are given in Table 1. As shown in Figure 6 and Table 1, 10 kinds of organosulfates were successfully detected and identified from cyclohexene SOA. The result not only first proved the formation of organosulfates from cyclohexene photooxidation at high-NO_x condition



with SO₂, but also provided evidence and reference for organosulfates identification by FTIR-IC joint technique. A deprotonated molecular ion at $m/z=195.03322$ (C₆H₁₁O₅S⁻) had the maximum content (more than 60%) of all the organosulfates detected in our study. Its intensity was 6.5 times higher than that of the second highest abundant organosulfate. The intermediate product of cyclohexene with OH, i.e., CH(O)CH₂CH₂CH₂CH₂CHOH, has a hydroxyl group, and the organosulfate product ($m/z=195.03322$) might form from the intermediate product, not from end product.

The mass spectra showed a great abundance of peaks, detected as deprotonated molecular ions (M-H)⁻ formed via proton abstraction. Most cyclohexene SOA contained carboxylic acid and/or aldehyde moieties. The products of the reaction of OH radicals with cyclohexene in the presence of NO were investigated and the products were identified as cyclic 1,2-hydroxynitrates and 1,6-hexanedial (Aschmann et al., 2012). These products couldn't be detected by ESI-HR-MS in our study. Aldehydes could be oxidized by OH radicals to form carboxyls, which have been intensively identified in previous studies (Cameron et al., 2002; Goldsmith et al., 2012). The 1,6-hexanedial might be further oxidized in the atmospheric photooxidation reactions to form the 1,6-adipic acid (C₆H₁₀O₄) and 6-oxohexanoic acid (C₆H₁₀O₃), which were both observed in our MS results. In addition to the C₆ compounds observed in this study, a C₅H₇O₃⁻ ion was detected with higher abundance than the C₆ compounds. Although the formation of this C₅ compound might be due to a carbonyl cleavage from a six-carbon atoms chain, a proper mechanism for its formation could not be determined. A C₄ compound was also detected in this study, likely as a result of a carbonyl cleavage from a C₅ compound. However, there was no evidence of the formation of compounds with less than four carbon atoms.

4 Conclusion

We report a series of chamber experiments studies on the formation of secondary aerosols from the mixture of cyclohexene and SO₂. The experiments were based on Fourier transform infrared spectrometer, ion chromatography and electrospray ionization high-resolution quadrupole mass spectrometer, and were performed under NO_x conditions. Although new particle formation was found to be enhanced with increasing SO₂ concentration, the yield of SOA was not enhanced for all SO₂ concentrations between 0 and 105 ppb. The SOA formation decreased at first and then was enhanced for all SO₂ concentration above 40 ppb.

Both acid-catalysis and competitive OH reactions with cyclohexene and SO₂ were found to have important effects on the SOA formation and hence, should be taken into account in SOA simulation models or air quality models for a better understanding of haze pollution. The formation of organosulfates, an important part of atmospheric organic aerosol components, was first observed from cyclohexene SOA. The formation of organosulfates has a great significance for the particulate matter formation under high SO₂ concentrations in the atmosphere.



Acknowledgments

This work was supported by National Natural Science Foundation of China (91644214, 21577080, 41375129), Shenzhen Science and Technology Research and Development Funds, China (JCYJ20150402105524052), and the “Strategic Priority Research Program (B)” of the Chinese Academy of Sciences (XDB05010104).

5 References

- Adams, J. M., Constable, J. V., Guenther, A. B., and Zimmerman, P.: An estimate of natural volatile organic compound emissions from vegetation since the last glacial maximum, *Chemosphere*, 3, 73-91, doi: 10.1016/S1465-9972(00)00023-4, 2001.
- Aschmann, S. M., Arey, J., and Atkinson, R.: Kinetics and products of the reactions of OH radicals with cyclohexene, 1-methyl-1-cyclohexene, cis-cyclooctene, and cis-cyclodecene, *J. Phys. Chem. A*, 116, 9507-9515, doi: 10.1021/jp307217m, 2012.
- Atkinson, R.: Gas-phase tropospheric chemistry of volatile organic compounds: 1. Alkanes and alkenes, *J. Phys. Chem. Ref. Data*, 26, 215-290, doi: 10.1063/1.556012, 1997.
- Attwood, A., Washenfelder, R., Brock, C., Hu, W., Baumann, K., Campuzano-Jost, P., Day, D., Edgerton, E., Murphy, D., and Palm, B.: Trends in sulfate and organic aerosol mass in the southeast US: Impact on aerosol optical depth and radiative forcing, *Geophys. Res. Lett.*, 41, 7701-7709, doi: 10.1002/2014GL061669, 2014.
- Calvert, J. G., Su, F., Bottenheim, J. W., and Strausz, O. P.: Mechanism of the homogeneous oxidation of sulfur dioxide in the troposphere, *Atmos. Environ.*, 12, 197-226, doi: 10.1016/0004-6981(78)90201-9, 1978.
- Cameron, M., Sivakumaran, V., Dillon, T. J., and Crowley, J. N.: Reaction between OH and CH₃CHO. Part 1. Primary product yields of CH₃ (296 K), CH₃CO (296 K), and H (237-296 K), *Phys. Chem. Chem. Phys.*, 4, 3628-3638, doi: 10.1039/b202586h, 2002.
- Carlsson, P. T., Dege, J. E., Keunecke, C., Kruger, B. C., Wolf, J. L., and Zeuch, T.: Pressure dependent aerosol formation from the cyclohexene gas-phase ozonolysis in the presence and absence of sulfur dioxide: a new perspective on the stabilisation of the initial clusters, *Phys. Chem. Chem. Phys.*, 14, 11695-11705, doi: 10.1039/c2cp40714k, 2012.
- Chan, M. N., Surratt, J. D., Chan, A. W. H., Schilling, K., Offenberg, J. H., Lewandowski, M., Edney, E. O., Kleindienst, T. E., Jaoui, M., Edgerton, E. S., Tanner, R. L., Shaw, S. L., Zheng, M., Knipping, E. M., and Seinfeld, J. H.: Influence of aerosol acidity on the chemical composition of secondary organic aerosol from β -caryophyllene, *Atmos. Chem. Phys.*, 11, 1735-1751, doi: 10.5194/acp-11-1735-2011, 2011.
- Cheng, N., Zhang, D., Li, Y., Chen, T., Li, J., Dong, X., Sun, R., and Meng, F.: Analysis about spatial and temporal distribution of SO₂ and an ambient SO₂ pollution process in Beijing during 2000-2014, *Environ. Sci.*, 36, 3961-3971, doi: 10.13227/j.hjlx.2015.11.004, 2015.
- Chihara, G.: Characteristic infrared absorption band of organic sulfate esters, *Chem. Pharm. Bull.*, 6, 114, doi: 10.1248/cpb.6.114, 1958.
- Coury, C., and Dillner, A. M.: A method to quantify organic functional groups and inorganic compounds in ambient aerosols using attenuated total reflectance FTIR spectroscopy and multivariate chemometric techniques, *Atmos. Environ.*, 42, 5923-5932, doi: 10.1016/j.atmosenv.2008.03.026, 2008.
- Criegee, R.: Mechanism of ozonolysis, *Angew. Chem. Int. Edit.*, 14, 745-752, doi: 10.1002/anie.197507451, 1975.
- Darer, A. I., Cole-Filipiak, N. C., O'Connor, A. E., and Elrod, M. J.: Formation and stability of atmospherically relevant isoprene-derived organosulfates and organonitrates, *Environ. Sci. Technol.*, 45, 1895-1902, doi: 10.1021/es103797z, 2011.
- Du, L., Xu, Y. F., Ge, M. F., and Jia, L.: Rate constant for the reaction of ozone with diethyl sulfide, *Atmos. Environ.*, 41, 7434-7439, doi: 10.1016/j.atmosenv.2007.05.041, 2007.
- Edney, E., Kleindienst, T., Jaoui, M., Lewandowski, M., Offenberg, J., Wang, W., and Claeys, M.: Formation of 2-methyl tetrols and 2-methylglyceric acid in secondary organic aerosol from laboratory irradiated isoprene/NO_x/SO₂/air mixtures and their detection in ambient PM_{2.5} samples collected in the eastern United States, *Atmos. Environ.*, 39, 5281-5289, doi: 10.1016/j.atmosenv.2005.05.031, 2005.



- Emanuelsson, E. U., Watne, A. K., Lutz, A., Ljungstrom, E., and Hallquist, M.: Influence of humidity, temperature, and radicals on the formation and thermal properties of secondary organic aerosol (SOA) from ozonolysis of β -pinene, *J. Phys. Chem. A*, 117, 10346-10358, doi: 10.1021/jp4010218, 2013.
- 5 Froyd, K. D., Murphy, S. M., Murphy, D. M., de Gouw, J. A., Eddingsaas, N. C., and Wennberg, P. O.: Contribution of isoprene-derived organosulfates to free tropospheric aerosol mass, *Proc. Natl. Acad. Sci. U. S. A.*, 107, 21360-21365, doi: 10.1073/pnas.1012561107, 2010.
- Goldsmith, C. F., Green, W. H., and Klippenstein, S. J.: Role of $O_2 + QOOH$ in low-temperature ignition of propane. 1. Temperature and pressure dependent rate coefficients, *J. Phys. Chem. A*, 116, 3325-3346, doi: 10.1021/jp210722w, 2012.
- 10 Gomez-Gonzalez, Y., Surratt, J. D., Cuyckens, F., Szmigielski, R., Vermeylen, R., Jaoui, M., Lewandowski, M., Offenberg, J. H., Kleindienst, T. E., Edney, E. O., Blockhuys, F., Van Alsenoy, C., Maenhaut, W., and Claeys, M.: Characterization of organosulfates from the photooxidation of isoprene and unsaturated fatty acids in ambient aerosol using liquid chromatography/(-) electrospray ionization mass spectrometry, *J. Mass Spectrom.*, 43, 371-382, doi: 10.1002/jms.1329, 2008.
- Griffin, R. J., Cocker, D. R., Flagan, R. C., and Seinfeld, J. H.: Organic aerosol formation from the oxidation of biogenic hydrocarbons, *J. Geophys. Res.*, 104, 3555-3567, doi: 10.1029/1998jd100049, 1999.
- 15 Grosjean, D., Cauwenbergh, K. V., Schmid, J. P., Kelley, P. E., and Pitts, J. N.: Identification of C3-C10 aliphatic dicarboxylic acids in airborne particulate matter, *Environ. Sci. Technol.*, 12, 313-317, doi: 10.1021/es60139a005, 1978.
- Hansen, J. E., and Sato, M.: Trends of measured climate forcing agents, *Proc. Natl. Acad. Sci. U. S. A.*, 98, 14778-14783, doi: 10.1073/pnas.261553698, 2001.
- Hatch, L. E., Creamean, J. M., Ault, A. P., Surratt, J. D., Chan, M. N., Seinfeld, J. H., Edgerton, E. S., Su, Y. X., and Prather, K. A.: Measurements of isoprene-derived organosulfates in ambient aerosols by aerosol time-of-flight mass spectrometry-part 1: Single particle atmospheric observations in atlanta, *Environ. Sci. Technol.*, 45, 5105-5111, doi: 10.1021/es103944a, 2011.
- He, H., Wang, Y., Ma, Q., Ma, J., Chu, B., Ji, D., Tang, G., Liu, C., Zhang, H., and Hao, J.: Mineral dust and NOx promote the conversion of SO₂ to sulfate in heavy pollution days, *Sci. Rep.*, 4, 4172, doi: 10.1038/srep04172, 2014.
- 25 Hu, K. S., Darer, A. I., and Elrod, M. J.: Thermodynamics and kinetics of the hydrolysis of atmospherically relevant organonitrates and organosulfates, *Atmos. Chem. Phys.*, 11, 8307-8320, doi: 10.5194/acp-11-8307-2011, 2011.
- Iinuma, Y., Muller, C., Berndt, T., Boge, O., Claeys, M., and Herrmann, H.: Evidence for the existence of organosulfates from beta-pinene ozonolysis in ambient secondary organic aerosol, *Environ. Sci. Technol.*, 41, 6678-6683, doi: 10.1021/es070938t, 2007.
- 30 Jang, M., Czoschke, N. M., Lee, S., and Kamens, R. M.: Heterogeneous atmospheric aerosol production by acid-catalyzed particle-phase reactions, *Science*, 298, 814-817, doi: 10.1126/science.1075798, 2002.
- Jaoui, M., Kleindienst, T. E., Offenberg, J. H., Lewandowski, M., and Lonneman, W. A.: SOA formation from the atmospheric oxidation of 2-methyl-3-buten-2-ol and its implications for PM_{2.5}, *Atmos. Chem. Phys.*, 12, 2173-2188, doi: 10.5194/acp-12-2173-2012, 2012.
- 35 Jia, L., and Xu, Y. F.: Effects of relative humidity on ozone and secondary organic aerosol formation from the photooxidation of benzene and ethylbenzene, *Aerosol. Sci. Tech.*, 48, 1-12, doi: 10.1080/02786826.2013.847269, 2014.
- Jimenez, E., Gonzalez, S., Cazaunau, M., Chen, H., Ballesteros, B., Daele, V., Albaladejo, J., and Mellouki, A.: Atmospheric degradation initiated by OH radicals of the potential foam expansion agent, CF₃(CF₂)₂CH horizontal line CH₂ (HFC-1447fz): kinetics and formation of gaseous products and secondary organic aerosols, *Environ. Sci. Technol.*, 50, 1234-1242, doi: 10.1021/acs.est.5b04379, 2016.
- 40 Kalberer, M., Yu, J., Cocker, D. R., Flagan, R. C., and Seinfeld, J. H.: Aerosol formation in the cyclohexene-ozone system, *Environ. Sci. Technol.*, 34, 4894-4901, doi: 10.1021/es001180f, 2000.
- Kanakidou, M., Seinfeld, J. H., Pandis, S. N., Barnes, I., Dentener, F. J., Facchini, M. C., Van Dingenen, R., Ervens, B., Nenes, A., Nielsen, C. J., Swietlicki, E., Putaud, J. P., Balkanski, Y., Fuzzi, S., Horth, J., Moortgat, G. K., Winterhalter, R., Myhre, C. E. L., Tsigaridis, K., Vignati, E., Stephanou, E. G., and Wilson, J.: Organic aerosol and global climate modelling: a review, *Atmos. Chem. Phys.*, 5, 1053-1123, doi: 10.5194/acp-5-1053-2005, 2005.
- 45 Keywood, M. D., Varutbangkul, V., Bahreini, R., Flagan, R. C., and Seinfeld, J. H.: Secondary organic aerosol formation from the ozonolysis of cycloalkenes and related compounds, *Environ. Sci. Technol.*, 38, 4157-4164, doi: 10.1021/es035363o, 2004.



- Kristensen, K., and Glasius, M.: Organosulfates and oxidation products from biogenic hydrocarbons in fine aerosols from a forest in North West Europe during spring, *Atmos. Environ.*, **45**, 4546-4556, doi: 10.1016/j.atmosenv.2011.05.063, 2011.
- Lane, T. E., Donahue, N. M., and Pandis, S. N.: Effect of NO_x on secondary organic aerosol concentrations, *Environ. Sci. Technol.*, **42**, 6022-6037, doi: 10.1021/es703225a, 2008.
- 5 Lelieveld, J., and Heintzenberg, J.: Sulfate cooling effect on climate through in-cloud oxidation of anthropogenic SO₂, *Science*, **258**, 117-120, doi: 10.1126/science.258.5079.117, 1992.
- Lin, Y. H., Zhang, Z. F., Docherty, K. S., Zhang, H. F., Budisulistiorini, S. H., Rubitschun, C. L., Shaw, S. L., Knipping, E. M., Edgerton, E. S., Kleindienst, T. E., Gold, A., and Surratt, J. D.: Isoprene epoxydiols as precursors to secondary organic aerosol formation: acid-catalyzed reactive uptake studies with authentic compounds, *Environ. Sci. Technol.*, **46**, 250-258, doi: 10.1021/es202554c, 2012.
- 10 Liu, S., Shilling, J. E., Song, C., Hiranuma, N., Zaveri, R. A., and Russell, L. M.: Hydrolysis of organonitrate functional groups in aerosol particles, *Aerosol. Sci. Tech.*, **46**, 1359-1369, doi: 10.1080/02786826.2012.716175, 2012.
- Liu, T., Wang, X., Hu, Q., Deng, W., Zhang, Y., Ding, X., Fu, X., Bernard, F., Zhang, Z., and Lü, S.: Formation of secondary aerosols from gasoline vehicle exhausts when mixing with SO₂, *Atmos. Chem. Phys.*, **16**, 675-689, doi: 10.5194/acp-16-675-2016, 2016.
- 15 Lonsdale, C. R., Stevens, R. G., Brock, C. A., Makar, P. A., Knipping, E. M., and Pierce, J. R.: The effect of coal-fired power-plant SO₂ and NO_x control technologies on aerosol nucleation in the source plumes, *Atmos. Chem. Phys.*, **12**, 11519-11531, doi: 10.5194/acp-12-11519-2012, 2012.
- Mael, L. E., Jacobs, M. I., and Elrod, M. J.: Organosulfate and nitrate formation and reactivity from epoxides derived from 2-methyl-3-buten-2-ol, *J. Phys. Chem. A*, **119**, 4464-4472, doi: 10.1021/jp510033s, 2015.
- 20 McFiggans, G., Artaxo, P., Baltensperger, U., Coe, H., Facchini, M. C., Feingold, G., Fuzzi, S., Gysel, M., Laaksonen, A., Lohmann, U., Mentel, T. F., Murphy, D. M., O'Dowd, C. D., Snider, J. R., and Weingartner, E.: The effect of physical and chemical aerosol properties on warm cloud droplet activation, *Atmos. Chem. Phys.*, **6**, 2593-2649, doi: 10.5194/acp-6-2593-2006, 2006.
- 25 Nah, T., Sanchez, J., Boyd, C. M., and Ng, N. L.: Photochemical aging of alpha-pinene and beta-pinene secondary organic aerosol formed from nitrate radical oxidation, *Environ. Sci. Technol.*, **50**, 222-231, doi: 10.1021/acs.est.5b04594, 2016.
- Ofner, J., Kruger, H. U., Grothe, H., Schmitt-Kopplin, P., Whitmore, K., and Zetzsch, C.: Physico-chemical characterization of SOA derived from catechol and guaiacol-a model substance for the aromatic fraction of atmospheric HULIS, *Atmos. Chem. Phys.*, **11**, 1-15, doi: 10.5194/acp-11-1-2011, 2011.
- 30 Pandis, S. N., Paulson, S. E., Seinfeld, J. H., and Flagan, R. C.: Aerosol formation in the photooxidation of isoprene and β -pinene, *Atmos. Environ.*, **25**, 997-1008, doi: 10.1016/0960-1686(91)90141-S, 1991.
- Passananti, M., Kong, L. D., Shang, J., Dupart, Y., Perrier, S., Chen, J. M., Donaldson, D. J., and George, C.: Organosulfate formation through the heterogeneous reaction of sulfur dioxide with unsaturated fatty acids and long-chain alkenes, *Angew. Chem. Int. Edit.*, **55**, 10336-10339, doi: 10.1002/anie.201605266, 2016.
- 35 Pathak, R. K., Stanier, C. O., Donahue, N. M., and Pandis, S. N.: Ozonolysis of alpha-pinene at atmospherically relevant concentrations: Temperature dependence of aerosol mass fractions (yields), *J. Geophys. Res.*, **112**, doi: 10.1029/2006jd007436, 2007.
- Paulson, S. E., and Orlando, J. J.: The reactions of ozone with alkenes: An important source of HO_x in the boundary layer, *Geophys. Res. Lett.*, **23**, 3727-3730, doi: 10.1029/96GL03477, 1996.
- 40 Pokhrel, A., Kawamura, K., Ono, K., Seki, O., Fu, P. Q., Matoba, S., and Shiraiwa, T.: Ice core records of monoterpene- and isoprene-SOA tracers from Aurora Peak in Alaska since 1660s: Implication for climate change variability in the North Pacific Rim, *Atmos. Environ.*, **130**, 105-112, doi: 10.1016/j.atmosenv.2015.09.063, 2016.
- Pope III, C. A., and Dockery, D. W.: Health effects of fine particulate air pollution: lines that connect, *J. Air Waste Manage. Assoc.*, **56**, 709-742, doi: 10.1080/10473289.2006.10464485, 2006.
- 45 Presto, A. A., Hartz, K. E., and Donahue, N. M.: Secondary organic aerosol production from terpene ozonolysis. 1. Effect of UV radiation, *Environ. Sci. Technol.*, **39**, 7036-7045, doi: 10.1021/es050174m, 2005a.
- Presto, A. A., Hartz, K. E., and Donahue, N. M.: Secondary organic aerosol production from terpene ozonolysis. 2. Effect of NO_x concentration, *Environ. Sci. Technol.*, **39**, 7046-7054, doi: 10.1021/es050400s, 2005b.
- 50 Qi, L., Nakao, S., Tang, P., and Cocker, D. R.: Temperature effect on physical and chemical properties of secondary organic aerosol from m-xylene photooxidation, *Atmos. Chem. Phys.*, **10**, 3847-3854, doi: 10.5194/acp-10-3847-2010, 2010.



- Reddy, M. S., and Venkataraman, C.: Inventory of aerosol and sulphur dioxide emissions from India. Part II-biomass combustion, *Atmos. Environ.*, **36**, 699-712, doi: Doi 10.1016/S1352-2310(01)00464-2, 2002.
- Riva, M., Tomaz, S., Cui, T., Lin, Y. H., Perraudin, E., Gold, A., Stone, E. A., Villenave, E., and Surratt, J. D.: Evidence for an unrecognized secondary anthropogenic source of organosulfates and sulfonates: gas-phase oxidation of polycyclic aromatic hydrocarbons in the presence of sulfate aerosol, *Environ. Sci. Technol.*, **49**, 6654-6664, doi: 10.1021/acs.est.5b00836, 2015.
- 5 Riva, M., Budisulistiorini, S. H., Chen, Y., Zhang, Z., D'Ambro, E. L., Zhang, X., Gold, A., Turpin, B. J., Thornton, J. A., Canagaratna, M. R., and Surratt, J. D.: Chemical characterization of secondary organic aerosol from oxidation of isoprene hydroxyhydroperoxides, *Environ. Sci. Technol.*, **50**, 9889-9899, doi: 10.1021/acs.est.6b02511, 2016.
- 10 Romero, F., and Oehme, M.: Organosulfates – A new component of humic-like substances in atmospheric aerosols?, *J. Atmos. Chem.*, **52**, 283-294, doi: 10.1007/s10874-005-0594-y, 2005.
- Sakamoto, Y., Inomata, S., and Hirokawa, J.: Oligomerization reaction of the Criegee intermediate leads to secondary organic aerosol formation in ethylene ozonolysis, *J. Phys. Chem. A*, **117**, 12912-12921, doi: 10.1021/jp408672m, 2013.
- Sarrafzadeh, M., Wildt, J., Pullinen, I., Springer, M., Kleist, E., Tillmann, R., Schmitt, S. H., Wu, C., Mentel, T. F., and Zhao, D.: Impact of NO_x and OH on secondary organic aerosol formation from β-pinene photooxidation, *Atmos. Chem. Phys.*, **16**, 11237-11248, doi: 10.5194/acp-16-11237-2016, 2016.
- Sarwar, G., and Corsi, R.: The effects of ozone/limonene reactions on indoor secondary organic aerosols, *Atmos. Environ.*, **41**, 959-973, doi: 10.1016/j.atmosenv.2006.09.032, 2007.
- Shalamzari, M. S., Ryabtsova, O., Kahnt, A., Vermeylen, R., Herent, M. F., Quetin-Leclercq, J., Van der Veken, P., Maenhaut, W., and Claeys, M.: Mass spectrometric characterization of organosulfates related to secondary organic aerosol from isoprene, *Rapid Commun. Mass Spectrom.*, **27**, 784-794, doi: 10.1002/rcm.6511, 2013.
- Sihto, S. L., Kulmala, M., Kerminen, V. M., Dal Maso, M., Petaja, T., Riipinen, I., Korhonen, H., Arnold, F., Janson, R., Boy, M., Laaksonen, A., and Lehtinen, K. E. J.: Atmospheric sulphuric acid and aerosol formation: implications from atmospheric measurements for nucleation and early growth mechanisms, *Atmos. Chem. Phys.*, **6**, 4079-4091, doi: 10.5194/acp-6-4079-2006, 2006.
- 25 Sipilä, M., Berndt, T., Petaja, T., Brus, D., Vanhanen, J., Stratmann, F., Patokoski, J., Mauldin, R. L., III, Hyvarinen, A. P., Lihavainen, H., and Kulmala, M.: The role of sulfuric acid in atmospheric nucleation, *Science*, **327**, 1243-1246, doi: 10.1126/science.1180315, 2010.
- Sipilä, M., Jokinen, T., Berndt, T., Richters, S., Makkonen, R., Donahue, N. M., Mauldin, R. L., III, Kurten, T., Paasonen, P., and Samela, N.: Reactivity of stabilized Criegee intermediates (sCI) from isoprene and monoterpene ozonolysis toward SO₂ and organic acids, *Atmos. Chem. Phys.*, **14**, 3071-3098, doi: 10.5194/acpd-14-3071-2014, 2013.
- Somnitz, H.: Quantum chemical and dynamical characterisation of the reaction OH+SO₂⇌HOSO₂ over an extended range of temperature and pressure, *Phys. Chem. Chem. Phys.*, **6**, 3844-3851, doi: 10.1039/b317055a, 2004.
- 30 Song, C., Na, K., and Cocker, D. R., 3rd: Impact of the hydrocarbon to NO_x ratio on secondary organic aerosol formation, *Environ. Sci. Technol.*, **39**, 3143-3149, doi: 10.1021/es0493244, 2005.
- 35 Staudt, S., Kundu, S., Lehmler, H. J., He, X., Cui, T., Lin, Y. H., Kristensen, K., Glasius, M., Zhang, X., Weber, R. J., Surratt, J. D., and Stone, E. A.: Aromatic organosulfates in atmospheric aerosols: synthesis, characterization, and abundance, *Atmos. Environ.*, **94**, 366-373, doi: 10.1016/j.atmosenv.2014.05.049, 2014.
- Stewart, D. J., Almabrok, S. H., Lockhart, J. P., Mohamed, O. M., Nutt, D. R., Pfrang, C., and Marston, G.: The kinetics of the gas-phase reactions of selected monoterpenes and cyclo-alkenes with ozone and the NO₃ radical, *Atmos. Environ.*, **70**, 227-235, doi: 10.1016/j.atmosenv.2013.01.036, 2013.
- Sun, H., Li, S., Zhang, Y., Jiang, H., Qu, L., Liu, Z., and Liu, S.: Selective hydrogenation of benzene to cyclohexene in continuous reaction device with two reaction reactors in serie over Ru-Co-B/ZrO₂ catalysts, *Chin. J. Catal.*, **34**, 1482-1488, doi: 10.1016/S1872-2067(12)60637-8, 2013.
- 45 Surratt, J. D., Kroll, J. H., Kleindienst, T. E., Edney, E. O., Claeys, M., Sorooshian, A., Ng, N. L., Offenberg, J. H., Lewandowski, M., Jaoui, M., Flagan, R. C., and Seinfeld, J. H.: Evidence for organosulfates in secondary organic aerosol, *Environ. Sci. Technol.*, **41**, 517-527, doi: 10.1021/es062081q, 2007.
- Surratt, J. D., Gomez-Gonzalez, Y., Chan, A. W., Vermeylen, R., Shahgholi, M., Kleindienst, T. E., Edney, E. O., Offenberg, J. H., Lewandowski, M., Jaoui, M., Maenhaut, W., Claeys, M., Flagan, R. C., and Seinfeld, J. H.: Organosulfate formation in biogenic secondary organic aerosol, *J. Phys. Chem. A*, **112**, 8345-8378, doi: 10.1021/jp802310p, 2008.
- 50



- Tolocka, M. P., and Turpin, B.: Contribution of organosulfur compounds to organic aerosol mass, *Environ. Sci. Technol.*, **46**, 7978-7983, doi: 10.1021/es300651v, 2012.
- Wang, X. K., Rossignol, S., Ma, Y., Yao, L., Wang, M. Y., Chen, J. M., George, C., and Wang, L.: Identification of particulate organosulfates in three megacities at the middle and lower reaches of the Yangtze River, *Atmos. Chem. Phys.*, **15**, 21415-21448, doi: 10.5194/acpd-15-21415-2015, 2015.
- 5 Wang, X. M., Carmichael, G., Chen, D. L., Tang, Y. H., and Wang, T. J.: Impacts of different emission sources on air quality during March 2001 in the Pearl River Delta (PRD) region, *Atmos. Environ.*, **39**, 5227-5241, doi: 10.1016/j.atmosenv.2005.04.035, 2005.
- 10 Warren, B., Malloy, Q. G. J., Yee, L. D., and Cocker, D. R.: Secondary organic aerosol formation from cyclohexene ozonolysis in the presence of water vapor and dissolved salts, *Atmos. Environ.*, **43**, 1789-1795, doi: 10.1016/j.atmosenv.2008.12.026, 2009.
- Wu, L. Y., Tong, S. R., Zhou, L., Wang, W. G., and Ge, M. F.: Synergistic Effects between SO₂ and HCOOH on α -Fe₂O₃, *J. Phys. Chem. A*, **117**, 3972-3979, doi: 10.1021/jp400195f, 2013.
- 15 Xiao, S., Wang, M. Y., Yao, L., Kulmala, M., Zhou, B., Yang, X., Chen, J. M., Wang, D. F., Fu, Q. Y., Worsnop, D. R., and Wang, L.: Strong atmospheric new particle formation in winter in urban Shanghai, China, *Atmos. Chem. Phys.*, **15**, 1769-1781, doi: 10.5194/acp-15-1769-2015, 2015.
- Xu, W., Gomez-Hernandez, M., Guo, S., Secrest, J., Marrero-Ortiz, W., Zhang, A. L., and Zhang, R.: Acid-catalyzed reactions of epoxides for atmospheric nanoparticle growth, *J. Am. Chem. Soc.*, **136**, 15477-15480, doi: 10.1021/ja508989a, 2014.
- 20 Zhang, H., Worton, D. R., Lewandowski, M., Ortega, J., Rubitschun, C. L., Park, J. H., Kristensen, K., Campuzano-Jost, P., Day, D. A., Jimenez, J. L., Jaoui, M., Offenberg, J. H., Kleindienst, T. E., Gilman, J., Kuster, W. C., de Gouw, J., Park, C., Schade, G. W., Frossard, A. A., Russell, L., Kaser, L., Jud, W., Hansel, A., Cappellin, L., Karl, T., Glasius, M., Guenther, A., Goldstein, A. H., Seinfeld, J. H., Gold, A., Kamens, R. M., and Surratt, J. D.: Organosulfates as tracers for secondary organic aerosol (SOA) formation from 2-methyl-3-buten-2-ol (MBO) in the atmosphere, *Environ. Sci. Technol.*, **46**, 9437-9446, doi: 25 10.1021/es301648z, 2012.
- Zhang, H., Zhang, Z., Cui, T., Lin, Y. H., Bhathela, N. A., Ortega, J., Worton, D. R., Goldstein, A. H., Guenther, A., Jimenez, J. L., Gold, A., and Surratt, J. D.: Secondary organic aerosol formation via 2-Methyl-3-buten-2-ol photooxidation: evidence of acid-catalyzed reactive uptake of epoxides, *Environ. Sci. Technol. Lett.*, **1**, 242-247, doi: 10.1021/ez500055f, 2014.
- 30 Zhang, X., Schwantes, R. H., McVay, R. C., Lignell, H., Coggon, M. M., Flagan, R. C., and Seinfeld, J. H.: Vapor wall deposition in Teflon chambers, *Atmos. Chem. Phys.*, **15**, 4197-4214, doi: 10.5194/acp-15-4197-2015, 2015.
- Zielinska, B., Sagebiel, J. C., Harshfield, G., Gertler, A. W., and Pierson, W. R.: Volatile organic compounds up to C₂₀ emitted from motor vehicles; measurement methods, *Atmos. Environ.*, **30**, 2269-2286, doi: 10.1016/1352-2310(95)00116-6, 1996.

35

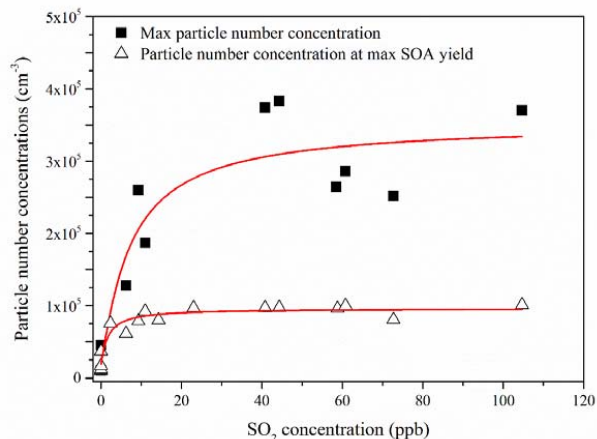


Figure 1: Particle number concentrations for cyclohexene/NO_x/SO₂ system with different initial SO₂ concentrations.

5

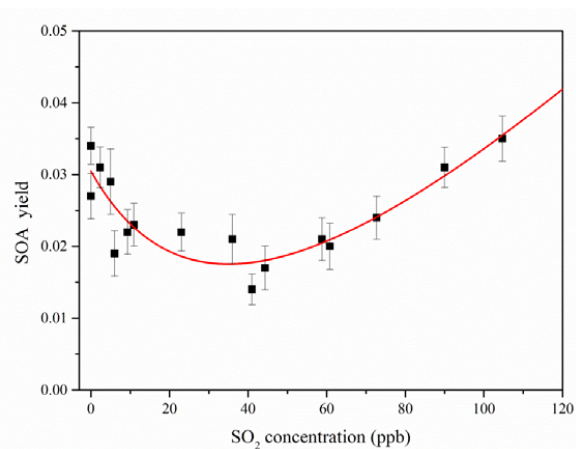


Figure 2: SOA yields of cyclohexene photooxidation in the presence of NO_x at different initial SO₂ concentrations. Solid line is least-square fitting to the data. The error bars were determined on the basis of propagation of uncertainties arising in the Δ H_C measurements, including GC calibration uncertainties propagation and the variance

10 in the initial cyclohexene measurements.

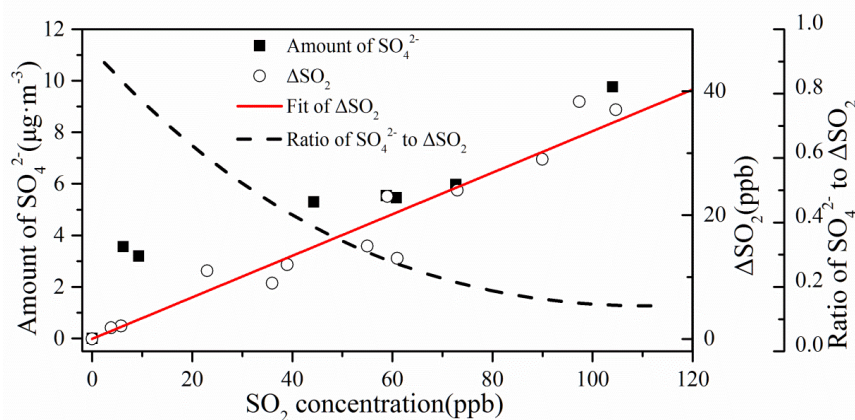


Figure 3: The amount of SO_4^{2-} in aerosols, consumption of SO_2 (ΔSO_2) and the ratio of the amount of SO_2 for SO_4^{2-} formation to ΔSO_2 with different initial SO_2 concentrations.

5

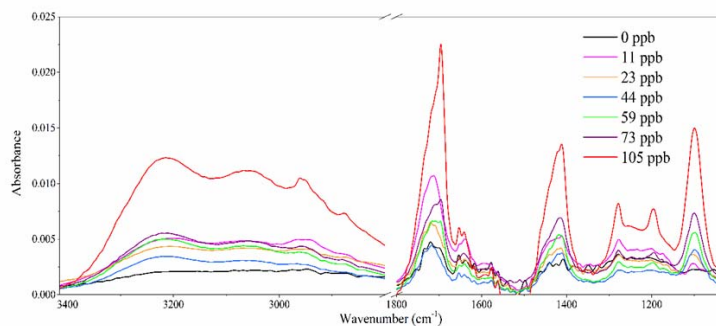


Figure 4: IR spectra of aerosols from cyclohexene/NOx/SO₂ system under different SO₂ concentrations.

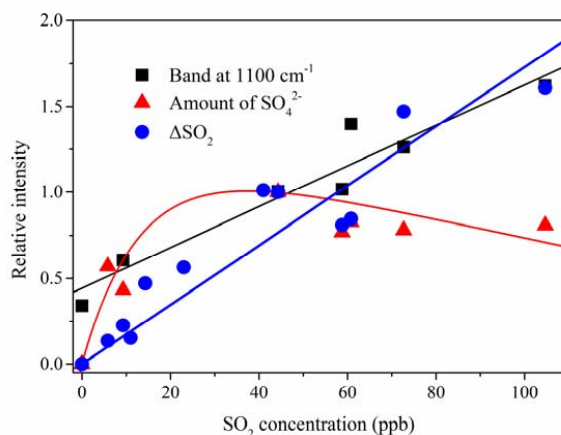


Figure 5: The relative intensity of the band at 1100 cm^{-1} (square), the amount of SO_4^{2-} (triangle) and ΔSO_2 (circle) of unit mass of aerosols. The relative intensity was set to 1 when the initial SO_2 concentration was 44.3 ppb .

5

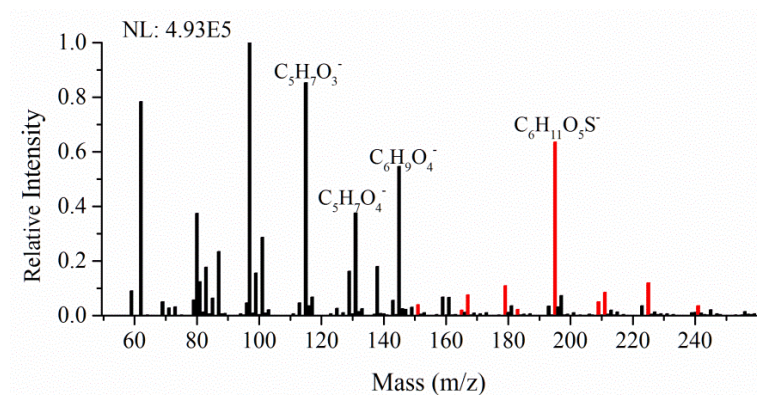


Figure 6: Negative ion mode ESI mass spectrum of SOA generated from the photooxidation of cyclohexene in the presence of SO_2 . Red peaks correspond to formulae containing sulfonic acid group. The mass resolution is 10^5 .

10



Table 1. Accurate mass fittings for main products and measured organosulfates ions in ESI negative ion mode from cyclohexene photooxidation in the presence of SO₂ under high-NO_x conditions

Measured ^a m/z	Ion	Proposed Ion Formula	Delta ^b (ppm)	RDB ^c
115.03942		C ₅ H ₇ O ₃ ⁻	-5.628	2
145.05019		C ₆ H ₉ O ₄ ⁻	-3.048	2
131.03444		C ₅ H ₇ O ₄ ⁻	-4.136	2
101.06006	(M-H) ⁻	C ₅ H ₉ O ₂ ⁻	-7.351	1
87.04433		C ₄ H ₇ O ₂ ⁻	-9.453	1
129.05515		C ₆ H ₉ O ₃ ⁻	-4.397	2
99.04439		C ₅ H ₇ O ₂ ⁻	-7.702	2
Organosulfates				
195.03322		C ₆ H ₁₁ O ₅ S ⁻	-0.243	1
225.00771		C ₆ H ₉ O ₇ S ⁻	1.171	2
179.00181		C ₅ H ₇ O ₅ S ⁻	-0.0879	2
211.02828		C ₆ H ₁₁ O ₆ S ⁻	0.464	1
167.00167	(M-H) ⁻	C ₄ H ₇ O ₅ S ⁻	-1.780	1
209.01257		C ₆ H ₉ O ₆ S ⁻	0.182	2
151.00658		C ₄ H ₇ O ₄ S ⁻	-3.130	1
241.00278		C ₆ H ₉ O ₈ S ⁻	1.738	2
182.99667		C ₄ H ₇ O ₆ S ⁻	-1.158	1
164.98594		C ₄ H ₅ O ₅ S ⁻	-2.287	2

^a Sort by abundance intensity.

^b Delta: label the peak with the difference between the theoretical and measured m/z.

^c RDB: ring and double bond equivalent.